

THE DEPENDENCE OF RAPIDITY AND CENTRALITY ON DIRECTED FLOW FROM AU+AL EVENTS

RACHEL DOMAGALSKI

ABSTRACT. At RHIC, many Au+Al events have been recorded at STAR from gold beams with low injection energy crashing into the aluminum beam pipe. Glauber modeling has been applied to determine centrality from pion multiplicity. The event plane method has been used to show that directed flow increases with rapidity. Fitting the Fourier series of the azimuthal distribution of particles yields results in agreement with the event plane method.

1. INTRODUCTION

The Relativistic Heavy Ion Collider (RHIC) has been used to create a quark-gluon plasma (QGP) by colliding the nuclei of gold atoms together at high energies [1]. Collisions where $\sqrt{s_{NN}}$ is from 7.7 GeV to 200 GeV have been extensively studied at RHIC. When Au+Au collisions of low center of mass energies were attempted at RHIC, the halo from the gold beam often collided with the aluminum beam pipe, creating fixed target Au+Al collisions where $\sqrt{s_{NN}} = 3, 3.5, \text{ and } 4.5$ GeV. The Solenoid Tracker at RHIC (STAR) has been able to select Au+Al collisions so they can be analyzed.

The first step of analyzing data from heavy ion collisions is to determine which events are closer to being more head-on, or central, as opposed to more peripheral collisions. This is achieved by comparing the results of Glauber Monte Carlo (GMC) simulations of events to actual data. What the GMC does is simulate heavy ion collisions and then gathers statistics from each event, such as the number of participating nucleons (N_{part}), the number of binary collisions (N_{coll}), and the distance from the centers of the two nuclei (b). Even though N_{part} , N_{coll} , and b cannot be measured directly, they can still be related to experimental data.

The motivation for separating the more central events from the more peripheral events is that different overlap regions of the heavy ion collisions should have different effects on the anisotropy after the collision. This is important for studying phenomena such as directed flow,

which is one type of anisotropic flow from heavy ion collisions. Directed flow represents a sideways flow of particles produced in heavy ion collisions in the Time Projection Chamber (TPC) at STAR.

2. THE GLAUBER MODEL FOR AU+AL COLLISIONS

The motivation for the GMC was to simulate the Au+Al collisions. The Glauber model was made in the standard GMC approach. First, the impact parameter gets chosen randomly. Next, the coordinates of the nucleons were randomly calculated with the Woods-Saxon function. After that, the inelastic nucleon-nucleon cross section was used to determine how many binary collisions took place and which nucleons were colliding. The results of the GMC calculations were then used to determine centrality of the fixed target collisions.

2.1. The Impact Parameter. The impact parameter, denoted as b , is defined as the distance between the centers of the two nuclei in the collision. In nuclear collisions, the occurrence of head-on collisions is rare, while peripheral collisions are more likely. The impact parameter in GMC calculations is chosen by treating the nuclear collision as randomly choosing the distance of some point in a circle. If a point inside a circle of radius R is randomly chosen, the probability that it will be located somewhere in a ring of width dr at a distance $r \leq R$ from the center of the circle is $2\pi r dr$. Thus, the impact parameter is chosen from a linear distribution.

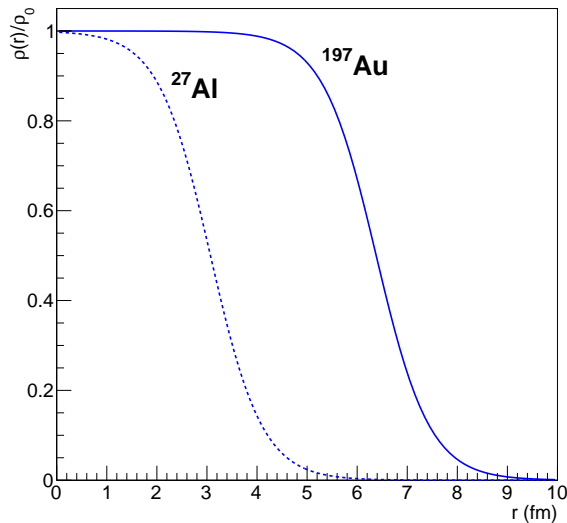


FIGURE 1. Radial density functions for gold and aluminum.

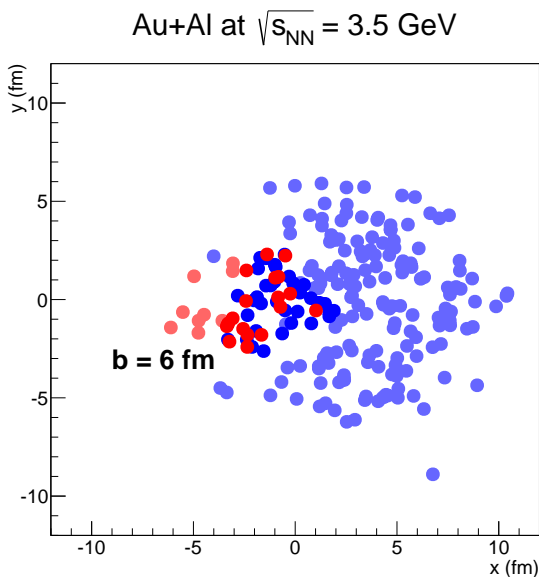


FIGURE 2. Au+Al collision at $\sqrt{s_{NN}} = 3.5$ GeV. Participating Au (blue) and Al (red) nucleons are highlighted.

2.2. The Woods-Saxon function. For spherical nuclei, the two-parameter Woods-Saxon density function is defined as [2]

$$\rho(r) = \rho_0 \cdot \frac{1 + w(r/R)^2}{1 + \exp((r - R)/a)} \quad (1)$$

for a nucleus of central density ρ_0 . The main parameters are the nuclear radius (R), and the nuclear skin thickness (a). The parameter w is related to the spherical symmetry of the nucleus and is zero for both gold and aluminum. In the GMC approach, one assigns the distance of a nucleon from the center of the nucleus by randomly choosing from the distribution $r^2\rho(r)$. The angular coordinates of each nucleon were taken randomly from the distributions φ and $\cos(\theta)$. The parameters for gold are $R = 6.38$ fm and $a = 0.535$ fm [3]. For aluminum, the parameters are $R = 3.07$ fm and $a = 0.519$ fm [4].

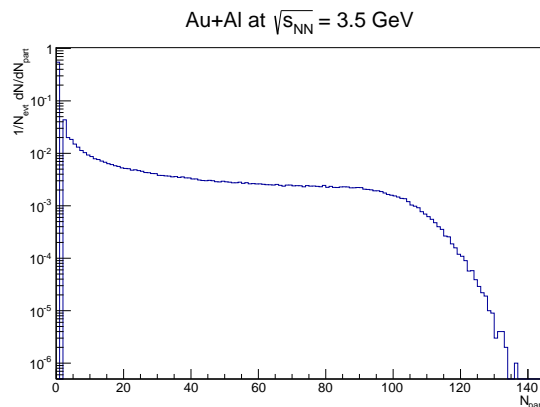


FIGURE 3. Results of N_{part} from many GMC simulations of Au+Al collisions at $\sqrt{s_{NN}} = 3.5$ GeV.

2.3. The Inelastic Cross Section. In order to determine whether or not two nucleons collide, one must know the inelastic nucleon-nucleon cross sectional area (σ_{inel}^{NN}), which varies with $\sqrt{s_{NN}}$. At $\sqrt{s_{NN}} = 200$ GeV, $\sigma_{NN} = 42$ mb [2]. In the fixed target collisions where $\sqrt{s_{NN}}$ was 3-4.5 GeV, $\sigma_{inel}^{NN} = 30$ mb [5]. If the distance in the x-y plane of two nucleons in the different nuclei was at

$$d \leq \sqrt{\sigma_{inel}^{NN}/\pi} \quad (2)$$

then the two nucleons participated in a binary collision [2]. In the Glauber Model, it is possible for one nucleon to participate in multiple binary collisions with no changes to the inelastic cross section. While there is a maximum number of participants independent of the inelastic cross section, the maximum number of collisions will

depend on the size of the cross section. The results of GMC simulations show that in Au+Al collisions, the maximum number of participants possible is never reached. This is because of the size difference between the gold and aluminum nuclei. In the most central collisions, all of the nucleons from aluminum will participate in binary collisions, but because of the size of the inelastic cross section, they cannot participate in binary collisions with all of the nucleons in the gold nucleus.

3. CENTRALITY IN FIXED TARGET AU+AL COLLISIONS

The motivation for defining centrality classes for nuclear collisions is that different overlap regions of the two nuclei produce different anisotropies. Additionally, N_{part} , N_{coll} , and b cannot be measured directly. However, such quantities can be related to charged-particle multiplicity and quantities such as $\langle N_{part} \rangle$ and $\langle N_{coll} \rangle$ can be calculated for each centrality class. The methods used to determine centrality in Au+Al collisions are very similar to those used in Au+Au collisions. However, in Au+Au collisions, centrality is determined by relating N_{part} to reference multiplicity, whereas in Au+Al collisions, the Glauber model is used to relate N_{part} to pion multiplicity.

3.1. The Negative Binomial Distribution.

In a sequence of independent Bernoulli trials where the probability of success in each trial is p , the negative binomial distribution (NBD) describes the probability of k failures occurring before r successes occur. The probability mass function of the NBD is defined as [6]

$$f(k) = \binom{k+r-1}{k} (1-p)^k p^r \quad (3)$$

where the mean of the NBD is $\mu = \frac{r(1-p)}{p}$. Alternatively, the NBD can be defined as

$$f(k) = \binom{k+r-1}{k} (1-p)^r p^k \quad (4)$$

where p represents the probability of failure in each trial. The mean of the second version of the NBD is $\mu = \frac{rp}{(1-p)}$. When writing the NBD in terms of its mean instead of p and extending

to real values of r , both versions of the NBD have the algebraic equivalency of [7]

$$f(k) = \frac{\Gamma(k+r)}{k!\Gamma(r)} \cdot \frac{(\mu/r)^k}{(1+\mu/r)^{k+r}}. \quad (5)$$

To avoid ambiguity, the parameters of (5) will be used as the parameters of the NBD. While it is unclear as to whether there is any physical significance of the negative binomial in nuclear collisions, it is a useful mathematical tool in relating the Glauber model to experimental data.

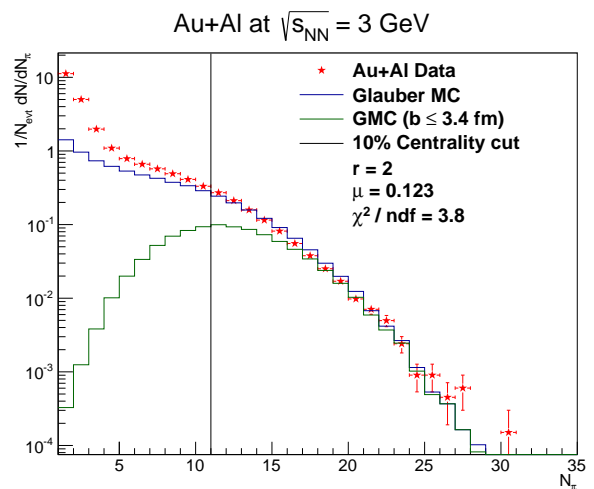


FIGURE 4. Negative Binomial fit for Au+Al at $\sqrt{s_{NN}} = 3$ GeV.

In Au+Au collisions, the reference multiplicity of each event can be determined from the Glauber model by summing N_{part} integers k drawn randomly from the NBD. This method can be applied to Au+Al collisions to find the pion multiplicity of each event. To determine the parameters, one must test for values of r and p that produce the best fit of the fixed target pion multiplicity data. The best fitting parameters of the NBD are the parameters that produce the histogram with the lowest χ^2 value with respect to the data.

3.2. Determining Centrality. To determine the compatibility of two histograms, one uses a χ^2 test. Two histograms that are very compatible with each other will have a χ^2 value close to 1. The χ^2 test is used to determine the parameters

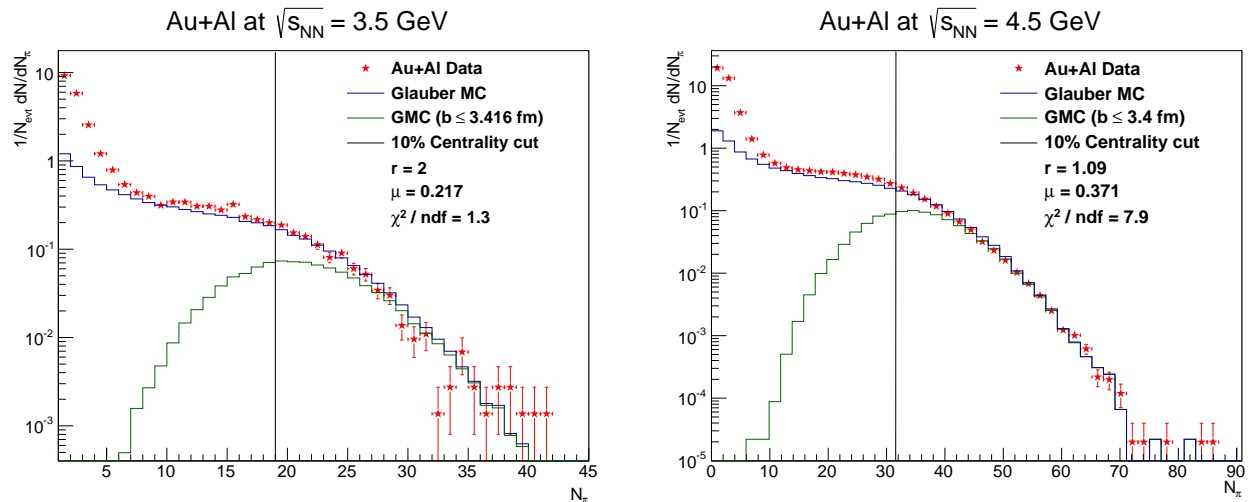


FIGURE 5. Negative Binomial fits for Au+Al at $\sqrt{s_{NN}} = 3.5$ GeV and $\sqrt{s_{NN}} = 4.5$ GeV.

of the NBD, which can then be used to determine centrality. This was done by producing histograms from the NBD with values of $0 < p < 1$ and $r \leq 10$ and testing them against the pion multiplicity data. To find the 10% centrality cut in pion multiplicity, one integrates 90% of the histogram filled from GMC data, then one does a χ^2 test in the tail of the histogram past the first 90% of the integral. The parameters that produce the χ^2 closest to 1 determine the cut in pion multiplicity. The 10% pion cut is the bin center at the first 90% of the integral of the GMC data. The directed flow analysis also requires the 5%, 20%, 30%, 40%, and 50% centrality cuts, which can be determined the same way as the 10% cut. The χ^2 test to compare histograms implemented by ROOT is a modified χ^2 based on a paper by N.D. Gagunashvili on comparing weighted and unweighted histograms [8].

3.3. Centrality Results. The methods for determining centrality as described above can find up to the 50% centrality cut. However, it is unclear as to whether events with pion multiplicities of less than 8 are actual Au+Al events. There are a couple of reasons as to why this happens. In any collision system and with any $\sqrt{s_{NN}}$ value, there is inefficiency in detecting peripheral collisions because the triggers in the STAR detector require that certain conditions

be met if an incoming particle is to be recorded. Also, when searching for candidates for potential Au+Al collisions, the STAR detector is essentially looking among background data. For events of low pion multiplicity, it is possible that the pions detected were not caused by Au+Al collisions. For example, an α particle could have collided into the aluminum beam pipe and produced an event of low pion multiplicity that could have passed the STAR triggers. Figures 4 and 5 show that STAR starts over-detecting Au+Al events when pion multiplicity is near 7 or 8 pions.

The directed flow analysis for each $\sqrt{s_{NN}}$ value will be done for centrality classes containing at least 8 pions. For $\sqrt{s_{NN}} = 3.5$ GeV, which had the best fit negative binomial, the flow analysis will be done on events containing a minimum of 7 pions. Table 1 lists the centrality cuts in pion multiplicity up to the 50% centrality cut.

TABLE 1. Pion multiplicity cuts for each centrality class.

$\sqrt{s_{NN}}$	3 GeV	3.5 GeV	4.5 GeV
5%	13	22	36
10%	11	19	31
20%	8	14	24
30%	6	10	16
40%	4	7	12
50%	3	4	8

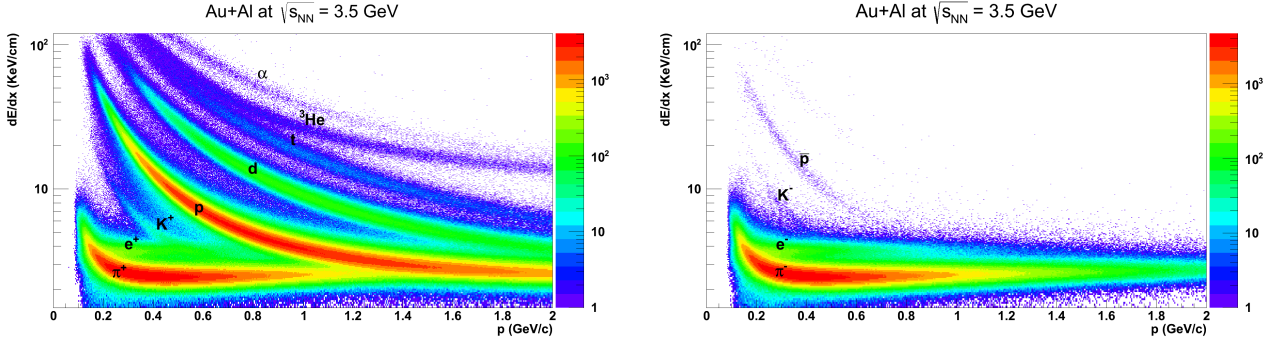


FIGURE 6. Particle identification plots for Au+Al at $\sqrt{s_{NN}} = 3.5$ GeV. Particle identification plots for $\sqrt{s_{NN}} = 3$ GeV and $\sqrt{s_{NN}} = 4.5$ GeV are highly similar. (left) Positively charged particles. (right) Negatively charged particles.

4. PARTICLE IDENTIFICATION

The relation used to find the rapidity of a relativistic particle is [3]

$$p_z = m_T \sinh y \quad (6)$$

where p_z is the momentum of the particle in the beam direction and m_T is the transverse mass of the particle. Since m_T depends on the type of the particle, particle identification is necessary in finding the rapidity of a particle. Particle identification is done by analyzing how a particle loses energy as it travels through the TPC as a function of its momentum. Each type of particle loses energy in the TPC differently, as shown by Figure 6. The curves in Figure 6 are the Bichsel curves for various types of particles. Each track in the TPC has a $n\sigma_\pi$ and $n\sigma_p$ value associated with it, which represents the distance of the particle on Figure 6 from the Bichsel functions of pions and protons, respectively. Positively charged particles and negatively charged particles are separated since the Bichsel functions of a particle and its antiparticle overlap.

One determines the type of particle first by filling histograms of the $n\sigma_\pi$ and $n\sigma_p$ and fitting a Gaussian to each histogram. For negatively charged particles, if a particle's $n\sigma_\pi$ value was within 3σ of the mean of the $n\sigma_\pi$ Gaussian fit, then the particle was identified as a π^- . For positively charged particles, if the $n\sigma_\pi$ value was within 2σ of the mean of the $n\sigma_\pi$ Gaussian and the particle's $n\sigma_p$ was less than negative one, the particle was identified as a π^+ . The reason that the $n\sigma_p$ value must be less than -1 for pion

identification is because at around $p > 1.2$, the regions around the Bichsel curves for pions and protons begin to overlap. If a particle's $n\sigma_p$ value was within 2σ of the mean of the $n\sigma_p$ Gaussian, the particle was identified as a proton.

5. FLOW ANALYSIS TECHNIQUES

The azimuthal distribution of particles is given by [9]

$$E \frac{d^3N}{d^3p} = \frac{1}{2\pi} \frac{d^2N}{p_T dp_T dy} \times \left(1 + 2 \sum_{n=1}^{\infty} v_n \cos(n(\phi - \Psi_{RP})) \right) \quad (7)$$

where E and p_T are the energy and transverse momentum of the particles. Each component v_n in the Fourier expansion represents some type of hydrodynamic flow. The component v_1 is what represents directed flow, which is the collective motion of particles in a sideways direction in the TPC. In Au+Au collisions, directed flow is zero at zero rapidity due to the symmetry of each event. Elliptic flow, v_2 , represents an elliptical expansion of particles in the $x - y$ plane. The Ψ_{RP} term in (7) is the reaction plane angle of the collision, which is the angle of the impact parameter in the $x - y$ plane. Since Ψ_{RP} cannot be directly measured, it must be approximated by the event plane. Once Ψ_{EP} , the estimation of Ψ_{RP} , is found for each event, the flow components can be calculated.

5.1. The Flow Vector. To find the event plane angle, Ψ_{EP} , one calculates the components of the

Q-vector [9] for each event and harmonic, defined as

$$Q_x = Q \cos(n\Psi_{EP}) = \sum_{i=1}^M w_i \cos(n\phi_i) \quad (8)$$

$$Q_y = Q \sin(n\Psi_{EP}) = \sum_{i=1}^M w_i \sin(n\phi_i)$$

where ϕ is the p_T angle measured in the TPC, M is the multiplicity of an event and the weight w_i is a function of rapidity and transverse momentum. Alternatively, one can calculate Ψ_{EP} directly from (8), since [9]

$$\Psi_{EP} = \frac{1}{n} \arctan \frac{\sum_{i=1}^M w_i \sin n(\phi_i)}{\sum_{i=1}^M w_i \cos n(\phi_i)}. \quad (9)$$

It can be seen from (9) that $0 \leq \Psi_{EP} \leq 2\pi/n$. Typically, different weights are used for even and odd n values [9].

5.2. The Event Plane Method. The definition of v_n in (7) is [9]

$$v_n \equiv \langle \cos(n(\phi - \Psi_{RP})) \rangle \quad (10)$$

where the average is taken over all tracks in a certain p_T or rapidity bin for a given centrality class. The event plane method uses Ψ_{EP} to find v_n by using (10) as [9]

$$v_n = \frac{1}{R} \langle \cos(n(\phi - \Psi_{EP})) \rangle \quad (11)$$

where R is the resolution of the event plane angle determined from (11). The resolution R is defined as [9]

$$R \equiv \langle \cos(n(\Psi_{EP} - \Psi_{RP})) \rangle \quad (12)$$

and is calculated by dividing each event into subevents [9]. The resolution of Au+Al events has not been calculated into this directed flow analysis.

5.3. Fitting the Fourier Series. Equation 7 describes the distribution of the p_T angles of particles with respect to the reaction planes of their events. From this, the event plane angle can be used to generate the azimuthal distribution of particles in momentum space. To find each v_n value, an azimuthal distribution of all tracks can be made for every rapidity and centrality bin. Figure 7 shows the distribution of π^- particles around midrapidity from events in the 10%-20% centrality bin. The very low points around $-\pi$

and π are due to binning in the histogram used to create Figure 7. Since the curve is proportional to $1 + 2 \sum_{n=1}^{\infty} v_n \cos(n(\phi - \Psi_{RP}))$, v_n can be easily found from the curve. Since Ψ_{EP} is used to generate the distribution, the same resolution parameter applied to (11) would be applied for the v_n values calculated by fitting the data.

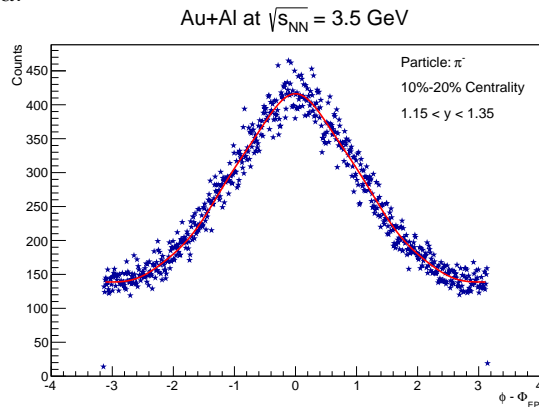


FIGURE 7. Fourier series fit to find v_1 value in a certain rapidity and centrality bin.

6. DIRECTED FLOW IN AU+AL COLLISIONS

Each v_n in (7) represents a different type of flow pattern of the anisotropy of the collision of the two nuclei. The v_n values describe the initial conditions after the collision has taken place. Directed flow, the type of flow described by v_1 , is the flow of particles to one side of the TPC. This analysis calculates directed flow as a function of rapidity and centrality. Figure 7 shows an example of a rapidity bin where v_1 is the dominant term in the Fourier expansion. This is different from Au+Au collisions where v_2 , elliptic flow, is the dominant type of flow after the collision.

6.1. Analysis. Since the flow analysis is on the dependence of rapidity of directed flow in Au+Al collisions, the weights in (8) were the rapidity values of each track. Another part of the weights came from the efficiency of the STAR detector. After particle identification was done, this efficiency was computed by taking the distribution of the lab angle ϕ for all detected tracks. The assumption was that the ϕ value with the most tracks, denoted as ϕ_{max} had 100% efficiency. The efficiency for each ϕ value was calculated as

the ratio of the number of tracks for that ϕ to the number of tracks of ϕ_{max} . The weight then was the rapidity value of the track divided by the efficiency of the azimuthal angle of the track. From this, the event plane angle for each event was calculated from (8) and (9). Once Ψ_{EP} was calculated for each track, (11) was used to calculate v_1 for each rapidity bin in each centrality class. In this analysis, v_1 was calculated separately for protons and pions.

The other method of calculating v_1 was from fitting the Fourier series of the azimuthal distribution of particles in a rapidity bin. In both the event plane method and with fitting the Fourier series, each rapidity bin was defined as rapidity values ± 0.1 from a central rapidity value. The functional form of the series in the code was $p_0 + p_1 \cos(x) + p_2 \cos(2x) + p_3 \cos(3x) + p_4 \cos(4x) + p_5 \cos(5x) + p_6 \cos(6x)$. To find v_1 from the fit, the parameter p_1 was divided by p_0 and again by 2 in accordance with (7). Figure 7 shows how the Fourier series was fit to the distribution of p_T angles.

6.2. Results. Figures 8 through 10 show the results of the analysis on directed flow. The analysis shows that in Au+Al fixed target collisions, directed flow increases with rapidity in all centrality classes. Additionally, the more peripheral collisions had larger v_1 values than the more central collisions. In Figures 8 through 10, the v_1 values at rapidity of -0.3 and 1.9 seemed to deviate from the trend in the rest of the data. This is most likely due to low statistics in those rapidity bins. When $-0.1 \leq y \leq 1.7$, the amount of particles used to determine v_1 was on the order of tens of thousands, while at the endpoints, the number of particles in those bins was on the order of thousands or even less than 1,000. In pions, v_1 followed a linear trend. In protons, the trend in v_1 was also linear, with an exception of when $\sqrt{s_{NN}}$ was 3 GeV. However, the higher the $\sqrt{s_{NN}}$, the more linear the trend was from the protons. While elliptic flow is the major component of flow in Au+Au collisions, it appears from Figure 7 that directed flow is the dominant component in Au+Al collisions away from zero rapidity.

The results in Figures 8 through 10 have not yet been corrected with the resolution of the

event plane. Typically, the resolution correction is done by dividing each event into three subevents based on pseudorapidity. The choice for subevents in Au+Au collisions is usually to have pseudorapidity bins for particles $-1 \leq \eta \leq -0.5$, $-0.5 \leq \eta \leq 0.5$, and $0.5 \leq \eta \leq 1$. In Au+Al collisions, the lowest η values were around -0.5, so the choices for subevents in Au+Au collisions does not hold over to the Au+Al data.

7. CONCLUSION

Using the negative binomial distribution with the Glauber Monte Carlo simulations to determine centrality from pion multiplicity was successful. The pion multiplicity distribution had a trend similar to N_{part} , which was used when sampling from the negative binomial. The analysis of directed flow showed that v_1 increased with rapidity, which was unexpected, since in Au+Au collisions, v_1 is negative when rapidity is positive [10]. While the results of the analysis were not what one would expect from Au+Au events, the two methods used to calculate directed flow agreed very well with each other.

8. FUTURE WORK

The resolution parameter (12) still needs to be found for the Au+Al collisions. Additionally, other methods of determining v_1 , such as the Lee-Yang zeros method can be used to compare with the event-plane method and the fit of the Fourier series. Also, fixed target collisions will continue to be studied, since there is an upcoming scheduled installation of a gold target at STAR [10].

9. ACKNOWLEDGMENTS

I would like to thank Daniel Cebra and Manuel Calderon for their mentorship over the summer. This project would not have been possible without their guidance. I would like to thank the UC Davis Nuclear Physics Group for their support and encouragement. I would like to thank Rena Zieve for directing an amazing REU program this summer. Finally, I would like to thank the National Science Foundation for funding the REU program.

APPENDIX A. THE NEGATIVE BINOMIAL

In Section 3.1, it was claimed that (3) and (5) are algebraically equivalent. The mean of (3) is

$$\mu = \frac{n(1-p)}{p}. \quad (13)$$

Solving for p yields $p = \frac{r}{r+\mu}$. Therefore,

$$(1-p)^k p^r = \left(1 - \frac{r}{r+\mu}\right)^k \left(\frac{r}{r+\mu}\right)^r. \quad (14)$$

Putting each term in (14) over a common denominator yields

$$(1-p)^k p^r = \left(\frac{\mu}{r+\mu}\right)^k \left(\frac{r}{r+\mu}\right)^r = \frac{\mu^k r^r}{(r+\mu)^{k+r}}. \quad (15)$$

Multiplying (15) by $\frac{r^{-k-r}}{r^{-k-r}}$ gives the result

$$(1-p)^k p^r = \frac{(\mu/r)^k}{(1+\mu/r)^{k+r}}. \quad (16)$$

The binomial coefficient in (3) can be rewritten with gamma functions as

$$\binom{k+r-1}{k} = \frac{\Gamma(k+r)}{k!\Gamma(r)}. \quad (17)$$

Putting together (16) and (17) demonstrates the equivalency of (3) and (5).

REFERENCES

- [1] M. Gyulassy. What have we learned at RHIC? *Journal of Physics G: Nuclear and Particle Physics*, 30(8):S911–S918, 2004.
- [2] S. J. Sanders M. L. Miller, K. Reygers and P. Steinberg. Glauber modeling in high energy nuclear collisions. *Annual Review of Nuclear and Particle Science*, 57:205–243, 2007.
- [3] R. Vogt. *Ultrarelativistic Heavy Ion Collisions*. Elsevier, 2007.
- [4] C. W. DeJager H. DeVries and C. DeVries. Nuclear charge density distribution parameters from elastic electron scattering. *Atomic Data and Nuclear Tables*, 36:495–536, 1987.
- [5] K. Nakamura. Review of particle physics. *Journal of Physics G: Nuclear and Particle Physics*, 37, 2010.
- [6] D. Prorok. Multiplicities in ultrarelativistic proton-(anti)proton collisions and negative binomial distribution fits. *International Journal of Modern Physics A*, 26(19):3171–3184, 2011.
- [7] P. Ghosh. Negative binomial multiplicity distribution in proton-proton collisions in limited pseudorapidity intervals at LHC up to $\sqrt{s} = 7$ tev and the clan model. arXiv:hep-ph/1202.4221v1, 2012.
- [8] R. Brun. The histogram classes, 2012. <http://root.cern.ch/root/html534/TH1.html>.
- [9] A. M. Posansker and S. A. Voloshin. Methods for analysing anisotropic flow in relativistic nuclear collisions. *Physical Review C*, 58(3):1671–1678, 1998.
- [10] Private communications with Daniel Cebra, UC Davis.

Au+Al at $\sqrt{s_{NN}} = 3.5$ GeV
Particle: π^-

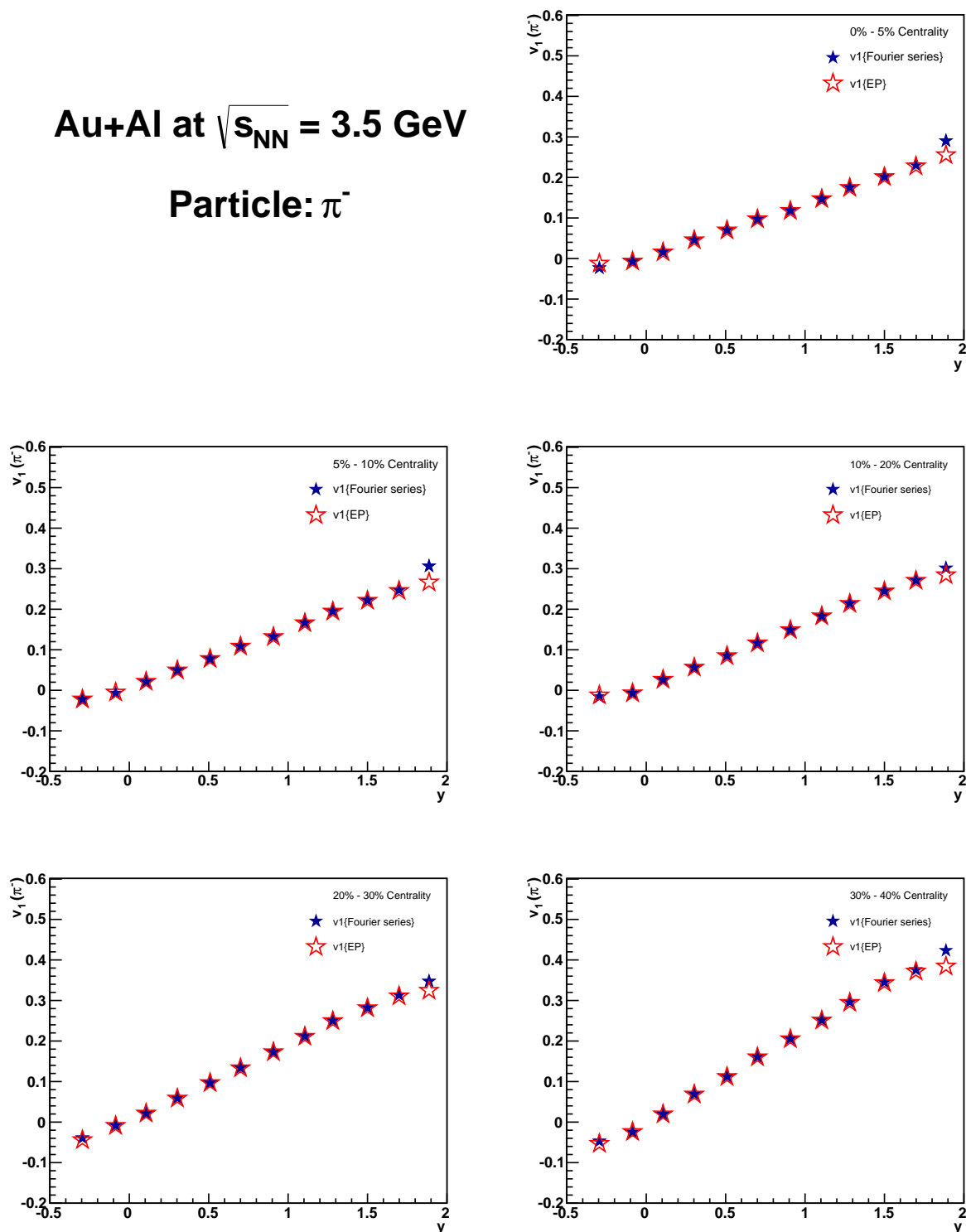


FIGURE 8. Directed flow from π^- particles at $\sqrt{s_{NN}} = 3.5$ GeV.

Au+Al at $\sqrt{s_{NN}} = 3.5$ GeV
Particle: π^+

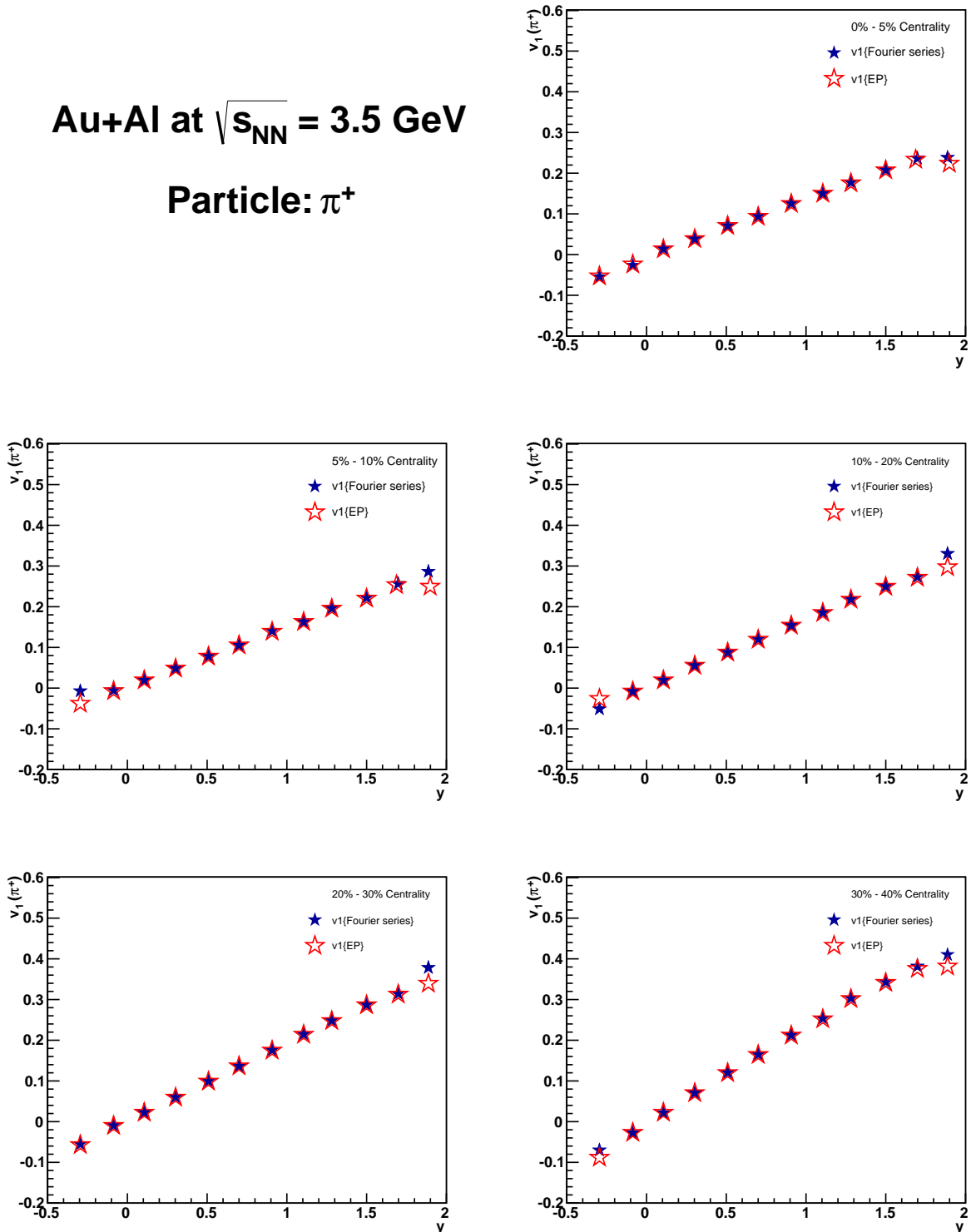


FIGURE 9. Directed flow from π^+ particles at $\sqrt{s_{NN}} = 3.5$ GeV.

Au+Al at $\sqrt{s_{NN}} = 3.5$ GeV
Particle: proton

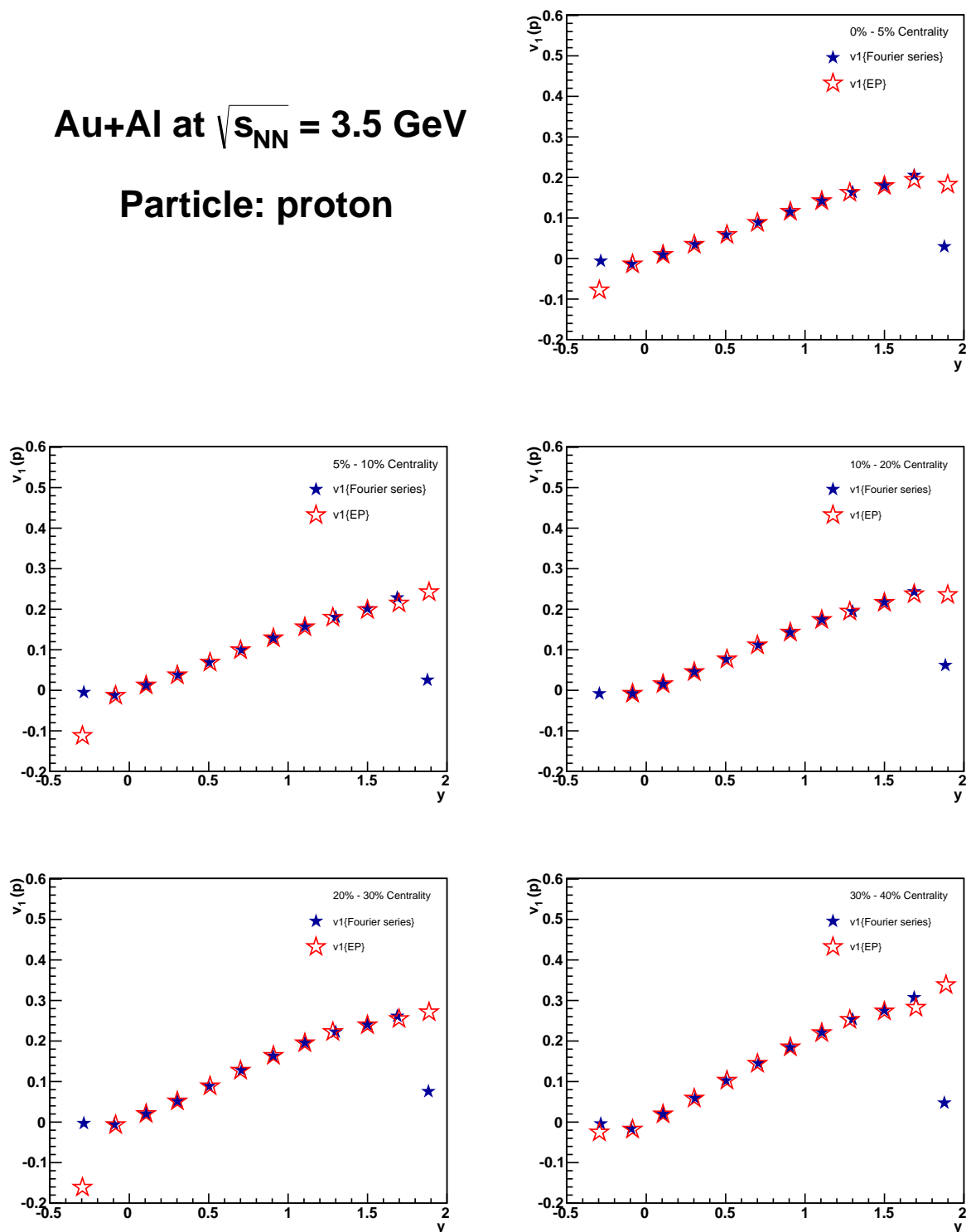


FIGURE 10. Directed flow from protons at $\sqrt{s_{NN}} = 3.5$ GeV.